

# Comparison of tunneling through molecules with Mott-Hubbard and with dimerization gaps

J. Favand<sup>a</sup> and F. Mila

Laboratoire de Physique Quantique, Université Paul Sabatier, 31062 Toulouse, France

Received: 17 November 1997 / Revised: 16 January 1998 / Accepted: 16 January 1998

**Abstract.** In order to study the tunneling of electrons through an interacting, 1D, dimerized molecule connected to leads, we consider the persistent current in a ring embedding this molecule. We find numerically that, for spinless fermions, a molecule with a gap mostly due to interactions, *i.e.* a Mott-Hubbard gap, gives rise to a larger persistent current than a molecule with the same gap, but due only to the dimerization. In both cases, the tunneling current decreases exponentially with the size of the molecule, but more slowly in the interacting case. Implications for molecular electronics are briefly discussed.

**PACS.** 73.40.Gk Tunneling – 73.61.Ph Polymers; organic compounds – 61.16.Ch Scanning probe microscopy; scanning tunneling, atomic force, scanning optical, magnetic force, etc.

## 1 Introduction

One of the major challenges of molecular electronics is to find molecules which could act as wires. For this purpose, special attention has been devoted to conjugated oligomers, and especially to the simplest of them, polyene, the finite size equivalent of polyacetylene ( $C_pH_{p+2}$ ). If one considers non-interacting particles, the conductance of the set lead-molecule-lead is, at low bias and according to Landauer's formula [1,2], proportional to the transmission coefficient through the molecule at the Fermi level of the leads. This approach was already successful in reproducing experimental results on a single  $C_{60}$  molecule [3], and it seems natural to apply it to polyene.

In the framework of non-interacting electrons, there is a charge gap due to the dimerization of the chain and Joachim and collaborators [4] found that the conductance shows a minimum when the Fermi energy of the leads is in the middle of this gap. At this point and only here, the current changes linearly with the voltage. Such a property is important to get a good molecular wire. Thus we have to consider the magnitude of the current at this point. Joachim showed that this minimum behaves as  $t_0 e^{-\gamma(2N-2)}$ ,  $2N$  being the length of the molecule. The coefficient  $\gamma$  grows with the dimerization, and the prefactor  $t_0$  depends on the lead-molecule contact. It turns out to be possible to tune these parameters to get non negligible currents in long wires (10 nm). These preliminary results were then confirmed by further simulations on polyenes and alkanes connected to golden leads. See also reference [5].

However, there are very good reasons to believe that electronic correlations play a role in fixing the magnitude of the charge gap in polyene [6]. We give here the main ones. First, the lowest excited state is dipole-allowed, and this can be recovered theoretically only when correlations are included [7]. Second, the observed negative spin densities [8,9] can be understood only for models with interaction [10]. Third, photo-induced absorption experiments [11] showing a splitting of the soliton peak in the middle of the gap would be puzzling without interactions [12]. Furthermore, *ab initio* calculations need to include in some way the correlation to get the right ground state dimerization [13]. Therefore, we wish to include interactions inside the molecule and treat them exactly. In comparison with the free case and for a given gap, we would like to know if these correlations increase or decrease the lowest current.

How can we study this current? Interesting results have been derived for a Luttinger liquid connected to leads [14,15], but they cannot be applied to the present case when the chemical potential lies in the gap. There is also a general formula describing the current through an interacting region connected to non-interacting leads [16]. However this formulation only allows an analytical evaluation if the interactions can be treated perturbatively, which is clearly not the case in polyene, and it is not so clear how to use numerical results obtained on finite size clusters for the Green's functions within this formalism.

So, we need another way to estimate the conductance. In the non-interacting case, the behavior of the conductance is strongly related to the exponential decrease of the amplitude of the wave function at the Fermi level inside the molecule. (We consider only one channel for simplicity.) This exponential decrease also controls the persistent current in a ring embedding the molecule. So, persistent

<sup>a</sup> e-mail: favand@irsamc2.ups-tlse.fr

currents and conductance are related in this case. We will assume that such a relationship still holds, at least qualitatively, in the interacting case. More precisely, we will suppose that what happens to the minimum persistent current by changing the molecular dimerization or interactions informs us on what would happen to the tunneling current, and we will concentrate on the persistent current because we know how to evaluate it numerically.

The paper is organized as follows. We introduce the model in Section 2. In Section 3, we analyze in more details the relationship between the persistent current and the conductance in the non-interacting case. Finally we present the central results of this paper about the persistent currents in the interacting case in Section 4.

## 2 The model

We describe the molecule by a dimerized and interacting region of length  $M$ . It is embedded in a non-interacting ring of length  $N$  describing the electrode (see Fig. 1). The ring is pierced by an Aharonov-Bohm flux  $\Phi$ . Denoting by  $L = N + M$  the total number of sites, the persistent current  $I(\Phi_0)$  is related to the groundstate energy  $E(\Phi)$  by  $I(\Phi_0) = L \frac{dE}{d\Phi} |_{\Phi=\Phi_0}$ . for simplicity we will concentrate on the mean value of  $|I|$  over  $\Phi_0$  given by  $\Delta I = \frac{L}{\pi} |E(\pi) - E(0)|$ .

We will use the following Hamiltonian:

$$\hat{H} = \hat{H}^e + \hat{H}^\alpha + \hat{H}^m + \hat{V} + \hat{\epsilon}_m \quad (1)$$

with

$$\begin{aligned} \hat{H}^e &= -t e^{i\phi} \sum_{i=0}^{N-2} c_{i+1}^\dagger c_i + h.c. \\ \hat{H}^\alpha &= (-\alpha e^{-i\phi} c_{L-1}^\dagger c_0 - \alpha e^{i\phi} c_N^\dagger c_{N-1}) + h.c. \\ \hat{H}^m &= -t_1 e^{i\phi} \sum_{i=0}^{M/2-1} c_{N+2i+1}^\dagger c_{N+2i} + h.c. \\ &\quad -t_2 e^{i\phi} \sum_{i=1}^{M/2-1} c_{N+2i}^\dagger c_{N+2i-1} + h.c. \\ \hat{V} &= V \sum_{i=N}^{L-2} n_i n_{i+1} \\ \hat{\epsilon}_m &= \epsilon_m \sum_{i=N}^{L-1} n_i. \end{aligned}$$

In these expressions, the operator  $c_j^\dagger$  creates a fermion at site  $j$ , and  $n_i = c_i^\dagger c_i$  is the density operator at site  $i$ . The metallic electrode is described by a tight-binding Hamiltonian  $\hat{H}^e$  with a hopping integral  $t$ .

The molecule is described by the sum of three terms:  $\hat{H}^m$  is a tight-binding Hamiltonian that describes the kinetic energy inside the molecule. It involves two alternating hopping integrals  $t_1$  and  $t_2$  to take the dimerization

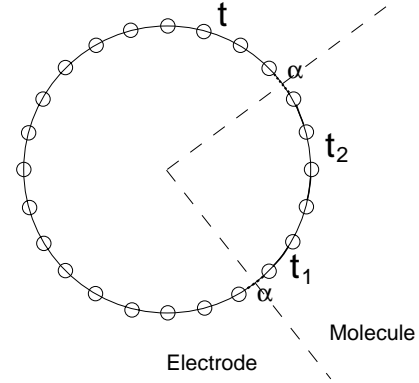


**Fig. 1.** Geometry of the system. Each open circle corresponds to a site and the links correspond to the various hopping integrals.

into account.  $\hat{V}$  represents the nearest neighbour repulsion between the particles, and  $\hat{\epsilon}_m$  fixes the chemical potential of the molecule.

The molecule and the electrode are connected by a transfer term  $\hat{H}^\alpha$  that allows the electrons to hop from one to the other.

Finally all the hopping integrals are multiplied by a phase factor  $e^{i\phi}$  with  $\phi = \Phi/L$  to describe the Aharonov-Bohm flux.

Of course a realistic calculation should deal with electrons, *i.e.* fermions with spin. It turns out however that the sizes one can reach with electrons are too small to allow a meaningful finite size analysis (see below). So we have decided to restrict ourselves to spinless fermions. This should be useful as a first step toward more realistic systems because the physics of Mott-Hubbard insulators — *i.e.* systems where the charge gap is due to correlations — is very similar for spinless fermions and fermions with spin.

## 3 Relationship between the persistent current and the conductance for non-interacting particles

There is no exact relation between the persistent current and the conductance in general, but we will show that the two quantities share qualitative and quantitative features in the non-interacting case.

### 3.1 How to calculate the conductance G?

According to Landauer, the conductance is proportional to the transmission coefficient  $T_F$  at the Fermi level. This coefficient can be calculated by considering two semi infinite leads connected to the molecule. Using the matching procedure, the stationary state  $|E\rangle$  of energy  $E$  can be searched for as:

$$\begin{aligned} |E\rangle &= |k_L^e\rangle + r_E | -k_L^e\rangle + A_1^m |k^m\rangle \\ &\quad + A_2^m | -k^m\rangle + t_E |k_R^e\rangle \end{aligned} \quad (2)$$

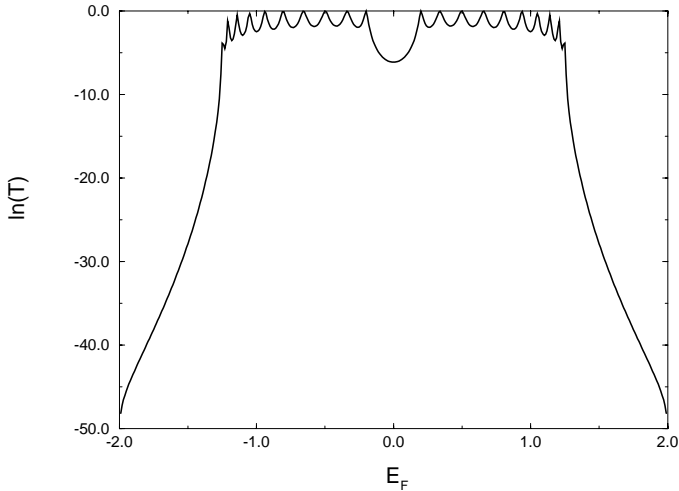


**Fig. 2.** Plot of the logarithm of the transmission coefficient  $T$  versus the Fermi energy  $E_F$  of the incident particle, in the non-interacting case. Here  $M = 20$ ,  $t_1 = 0.7t$ ,  $t_2 = 0.56t$ ,  $\alpha = 0.35t$ , in order to compare this plot to Joachim's result [3].

where  $r_E$ ,  $A_1^m$ ,  $A_2^m$  and  $t_E$  are unknown coefficients to be determined by continuity conditions. Here  $|k_{L,R}^e\rangle$  and  $|k^m\rangle$  correspond to the states with energy  $E$  that one would get for infinite leads or for an infinite molecule, and the momenta must satisfy:  $E = -2t \cos(k_j^e) = -\sqrt{t_1^2 + t_2^2 + 2t_1 t_2 \cos(2k_j^m)}$ . The transmission coefficient is then obtained as  $T(E) = |t_E|^2$ . An analytical formula for  $T(E)$  can be derived, but is too complicated to be written down. It is also possible to get  $T(E)$  for more realistic band structures. See reference [17]. A typical example is depicted in Figure 2. Although the method is different from that of reference [4], we have checked that the results are indeed the same.

### 3.2 How to calculate the persistent current $\Delta I$ ?

We now consider the geometry of Figure 1. In the absence of correlations, the total energy  $E$  inside the ring is the sum of the energies  $E_i$  of the occupied monoparticulate states (up to  $E_F$ ). Thus the total current  $I$  is the sum of the individual currents  $I_i$  of these levels.

The simplest way to get these energies  $E_i$  is again to use the matching procedure. The ring being closed, a monoparticulate state  $|E_i\rangle$  must now be searched for as:

$$|E_i\rangle = A_1^e |k_1^e\rangle + A_2^e |k_2^e\rangle + A_1^m |k_1^m\rangle + A_2^m |k_2^m\rangle \quad (3)$$

where  $|k_j^e\rangle$  and  $|k_j^m\rangle$  are again free propagating waves in the electrode and in the molecule. Note however that they now satisfy:  $E_i = -2t \cos(k_j^e - \phi) = -\sqrt{t_1^2 + t_2^2 + 2t_1 t_2 \cos(2k_j^m - 2\phi)}$ ,  $j = 1, 2$ , because of the Aharonov–Bohm flux.

The continuity conditions yield 4 linear equations for the coefficients  $A_i^e$  and  $A_i^m$ . We get a solution  $E_i$  each time

the determinant of this system vanishes. This determinant can be evaluated numerically, and we get the monoparticulate states and energies as in Section 3.1.

An alternative way consists in using the transfer matrix formalism. If  $\alpha$  and  $\beta$  are the amplitudes of the incoming and outgoing waves on the left side of the molecule, the incoming and outgoing amplitudes on the right side  $\alpha'$  and  $\beta'$  are given by

$$\begin{pmatrix} \beta' \\ \alpha' \end{pmatrix} = \begin{pmatrix} 1/t_k^* & -r_k^*/t_k^* \\ -r_k/t_k & 1/t_k \end{pmatrix} \begin{pmatrix} \alpha \\ \beta \end{pmatrix}$$

where  $t_k$  and  $r_k$  the transmission and reflection coefficients for an incident wave vector  $k$  defined in the preceding subsection. The matrix  $T_m$  that enters this equation is called the transfer matrix of the molecule.

A similar definition for the transfer matrix  $T_e$  of the electrode holds, with  $r_k = 0$  and  $t_k = e^{ikN}$ . The continuity conditions can then be written:

$$T_e \times T_m \begin{pmatrix} \alpha \\ \beta \end{pmatrix} = e^{i\Phi} \begin{pmatrix} \alpha \\ \beta \end{pmatrix}. \quad (4)$$

Note that in this approach the flux is concentrated in the boundary conditions, so that the energy is related to the wave-vectors by the usual relations of Section 3.1.

Denoting by  $\Theta_k$  the phase of  $t_k$ , the condition that the corresponding determinant vanishes yields:

$$|t_k| \cos(\Phi) = \cos(\Theta_k + kN) \quad (5)$$

This equation can be solved numerically for  $k$ ,  $t_k$  being calculated as in Section 2.1, and we get again the spectrum. While the matching procedure is more convenient for that purpose, this equation turns out to be very useful to discuss the minimum value of the persistent current as a function of the chemical potential  $\epsilon_m$  (see Sect. 3.4).

### 3.3 General shape of $G$ and $\Delta I$

We are now in a position to compare the behaviors of  $\Delta I$  and  $T$  with the Fermi level  $E_F$  of the electrode. More precisely, the important parameter is the difference  $E' = E_F - \epsilon_m$  which vanishes when  $E_F$  sits right in the middle of the molecular gap.

We can first control  $E'$  by varying the value of  $\epsilon_m$  for a given filling of the ring. The plot of  $\Delta I(E')$  for a half-filled system is given in Figure 3. Although their shape and size are modified, it is important to notice that the resonances are located at the same energies as for  $T(E_F)$ . Besides, as long as  $\alpha$  is not too large — which is the case in Figure 3 — the number of resonances is equal to  $M$  for both. Some of them are washed out — both for  $T$  and for  $\Delta I$  — when  $\alpha$  is of the order of  $t$  however.

We can also vary the filling  $N_F$  of the ring (which control  $E_F$ ) for a given  $\epsilon_m$ , say 0, and we get a similar result for  $\Delta I$  as a function of  $E'$  (See Fig. 3). The only difference is that some resonances are now missing since the bandwidth of the electrode is smaller than that of the molecule in the example of Figure 3. Of course they can all be restored by tuning the chemical potential of the molecule  $\epsilon_m$ .

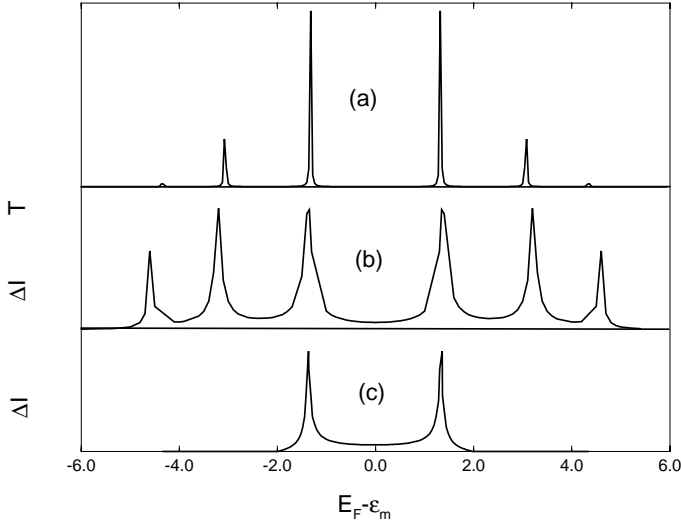


**Fig. 3.** Comparison of the transmission coefficient  $T$  and the average persistent current  $\Delta I$  in the non-interacting case for  $M = 6$ ,  $t_1 = 2.6t$ ,  $t_2 = 2.2t$ ,  $\alpha = 0.3t$ . (a)  $T$  versus the Fermi energy  $E_F$ . The on-site energy in the molecule  $\epsilon_m$  was set equal to zero. (b) Variation of  $\Delta I$  with  $E_F - \epsilon_m$  when  $E_F$  is fixed by the band filling and  $\epsilon_m$  varies. The parameters are  $N = 60$  and  $E_F = 0$  (half filling). (c) Variation of  $\Delta I$  with  $E_F - \epsilon_m$  when  $\epsilon_m$  is fixed and  $E_F$  varies with the filling. The parameters are  $\epsilon_m = 0$  and  $N = 120$ .

### 3.4 Value of the minimum current

We now compare the minimum value of the persistent current and the minimum value of the transmission coefficient. They both appear for  $E_F = 0$ , if the chemical potential of the molecule  $\epsilon_m$  is set to 0. Let us first calculate the mean current of the monoparticular state located at the Fermi level  $\Delta I_F = \frac{L}{\pi} |E_{k_F}(\Phi = \pi) - E_{k_F}(\Phi = 0)|$ . The energy at the Fermi level is given by:

$$E_F(\Phi) = -2t \cos[k_F(\Phi)]. \quad (6)$$

For a finite-size system,  $E_F < 0$  and  $|E_F| \ll 1$ , and equation (6) gives:

$$E_F(\Phi) = 2tk_F(\Phi) - t\pi. \quad (7)$$

We also know that  $|t_F(\Phi)| \ll 1$  and thus equation (5) yield:

$$Nk_F(\Phi) + \Theta_F(\Phi) = 2n\pi + \epsilon\pi/2 - \epsilon \cos\Phi |t_F(\Phi)| \quad (8)$$

where  $\epsilon = \pm 1$  and  $n \in \mathbb{Z}$  depend on  $N$  and the scattering properties of the molecule, but do not depend on  $\Phi$  since  $kN + \Theta_k$  is a continuous function of  $\Phi$ .

We get from equations (7, 8):

$$E_F(\Phi) = -2t[\Theta_F(\Phi) + 2n\pi + \epsilon\pi/2 - \epsilon \cos(\Phi)|t_F(\Phi)|]/N - t\pi. \quad (9)$$

Thus from equation (6) the current at the Fermi level is:

$$\Delta I_F = 2t[\epsilon(|t_F(\pi)| + |t_F(0)|) - \Theta_F(\pi) + \Theta_F(0)]L/N. \quad (10)$$

When  $N$  goes to infinity,  $N/L$  tends to 1,  $|t_F(\pi)|$  and  $|t_F(0)|$  merge and  $(\Theta_F(\pi) - \Theta_F(0))$  goes to zero.

Finally:

$$\Delta I_F = 4t\sqrt{T_F}. \quad (11)$$

It is possible to see in the same way that the sign of the current carried by the successive levels is alternate. The absolute value of this currents changes continuously with the energy level, and therefore at large  $L$ , the total current, which is the sum of the currents of the occupied level, is half of the last one. Thus, taking the absolute value:  $\Delta I = \Delta I_F/2$ .

So, by using the Landauer formula  $G = \frac{e^2}{h}T_F$ , we get the following relation between the persistent current and the conductance:

$$\Delta I = \frac{2t}{e}\sqrt{hG}.$$

The amplitude of a transmitted wave after the molecule is proportional to  $e^{-2\gamma M}$  with  $2 \cosh \gamma = t_1/t_2$ . Thus  $T_F$  and  $G$  decrease like  $e^{-2\gamma M}$  while  $\Delta I$  is proportional to  $e^{-\gamma M}$ . This point can be easily understood if we remember that we are free, by a gauge transformation, to concentrate the whole phase factor  $\Phi = \pi$  in the middle of the molecule. The difference between the zero flux case and the  $\Phi = \pi$  case in the Hamiltonian is  $\delta \hat{H} = 2 \times t_2(c_{\frac{M}{2}}^\dagger c_{\frac{M}{2}-1} + hc)$ . This can be seen as a perturbation and its first order influence on the level  $E_i$  is:

$$\delta E_i = \langle \Psi_i | \delta \hat{H} | \Psi_i \rangle = 2t_2[\Psi_i(M/2) \times \Psi_i^*(M/2 - 1) + cc].$$

At the Fermi level we have:  $\Psi_F(M/2) \propto e^{-\gamma M/2}$  and thus  $\delta E_F \propto e^{-\gamma M}$ . This energy shift is proportional to the Fermi-level current and thus to the total current.

As a conclusion, in the non-interacting case, the persistent current gives valuable informations on the conductance. First, the resonances have the same location. Second, the minimum persistent current is proportional to the square root of the minimum conductance. Thus, since the later decreases exponentially with the size of the molecule, the former has the same behavior, but with a coefficient in the exponential twice as small.

## 4 Persistent current for an interacting molecule

We now study the minimum persistent current in the ring when the interaction term  $\hat{V}$  is included. We have used three different methods to get the groundstate energy of the interacting system. The last two are mainly used to check the reliability of the first one.

### 4.1 Exact diagonalizations

We have used Lanczos algorithm to diagonalize the Hamiltonian and get the groundstate energy  $E_0(M, N)$  for small

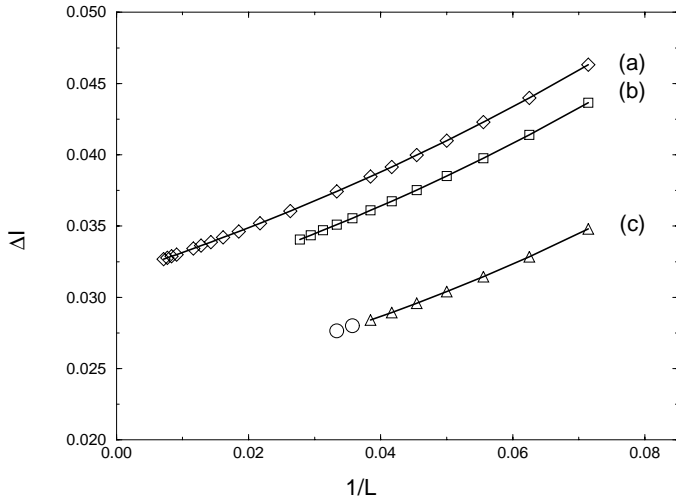


**Fig. 4.** Plot of the average persistent current  $\Delta I$  versus  $1/L$ . (a) Non-interacting case up to  $L = 140$  (diamonds). (b) First order perturbation according to equation (6) up to  $L = 36$  for  $V/t = 0.2$  (squares). (c) Exact diagonalizations up to  $L = 26$  (triangles) and DMRG for 28 and 30 sites (open circles) for  $V/t = 1$  and  $\epsilon_m/t = 0.76$ . In all cases a quadratic fit is correct. In this example  $M = 6$ ,  $t_1 = 2.6t$ ,  $t_2 = 2.2t$ ,  $\alpha = 0.3t$ .

values of  $M$  and  $N$ . For a given molecule of length  $M$ , we wish to get rid of the effect of the finite size  $N$  of the electrode. This was achieved by performing a finite size scaling on  $E(L)$  with fixed  $M$  and increasing  $N$ .

It turns out that a meaningful description for the molecule requires at least  $M = 6$ . Besides, to perform this scaling, we need as many values of  $N$  as possible, and this can be conveniently done while keeping the density fixed only at half-filling. Then for fermions with spin  $1/2$  and for  $L = 16$  the dimension of the Hilbert space is of the order of  $1.65 \times 10^8$ , *i.e.* too large to be handled numerically. Thus, in order to get enough points to perform a reliable finite size scaling, we have decided to limit our study to interacting spinless fermions. In that case, we could go up to  $L = 26$ , in which case the dimension of the Hilbert space is of the order of  $10^7$ .

If we plot the average persistent current *versus*  $1/L$ , it appears that a quadratic law fits the numerical results quite well (see Fig. 4) as long as the bandwidth of the electrode is smaller than the molecule's one. This case corresponds to a large enough density of states at the Fermi-energy of the electrode. To test the reliability of the fit, we have made the same plot up to  $L = 120$  for non-interacting particles (see also Fig. 4). The difference between the two extrapolated values for the two fits (up to  $L = 26$  and up to  $L = 120$ ) is never more than 5%. However, this is no proof that the same fit is accurate for interacting particles, and we now turn to alternative methods to check the extrapolation.

## 4.2 Small repulsion limit

We will now derive the persistent current to first order in the interaction  $V$ . Although this limit is not relevant for

the case of polyene, it will be used to test the reliability of our scaling law. The interaction term in the Hamiltonian is:

$$\hat{V} = V \sum_{i=0}^{M-2} c_i^\dagger c_i c_{i+1}^\dagger c_{i+1}.$$

The energy levels  $|E_j\rangle$  of the non-interacting case can be calculated as in Section 1.2. They are non-degenerate and form a basis for the monoparticular states. If the  $E_j$ 's are sorted in increasing order, the non-interacting ground state is given by:

$$|\Phi^0\rangle = \prod_{j \leq N_F} c_{E_j}^\dagger |\emptyset\rangle$$

where  $c_{E_j}^\dagger$  creates one particle in state  $|E_j\rangle$ . Besides, at half-filling,  $N_F = L/2$ . The original creation operator  $c_i^\dagger$  can then be written:

$$c_i^\dagger = \sum_{j=1}^N c_{E_j}^\dagger \langle E_j | i \rangle.$$

The first order correction to the ground state energy  $\Delta E = \langle \Phi^0 | \hat{V} | \Phi^0 \rangle$  is thus given by:

$$\Delta E = V \sum_{i=0}^{M-2} \left( \sum_{j \leq N_F, l \leq N_F} |\langle i+1 | E_j \rangle|^2 |\langle i | E_l \rangle|^2 \right. \\ \left. + \sum_{j \leq N_F, l > N_F} \langle E_j | i+1 \rangle \langle i+1 | E_l \rangle \langle E_l | i \rangle \langle i | E_j \rangle \right). \quad (12)$$

$\Delta E$  can be easily calculated numerically for periodic ( $\Phi = 0$ ) or antiperiodic ( $\Phi = \pi$ ) boundary conditions up to quite large systems. We can see in Figure 4 that the quadratic scaling law is still valid up to  $L = 36$  for small  $V$ .

## 4.3 DMRG

To find the ground state energy of a one-dimensional system, an alternative method to the exact diagonalisation is the Density Matrix Renormalisation Group [18]. While this method gives very precise results for open boundary conditions, it is always less accurate for closed boundary conditions.

Treating the molecule exactly and considering half of the electrode as the growing block, we meet strong limitations. Indeed, if  $M = 6$ , adding 1 site at each junction between the molecule and the leads to avoid artefacts and 2 sites to let the system grow, we have to treat 10 sites exactly. If we keep  $m = 100$  states to describe this growing block, the dimension  $d$  of the global Hilbert space is roughly:  $d = m \times 2^{10} \times m = 10^7$  and it is difficult to do much better.

Therefore, we have only been able to get accurate results up to  $L = 30$ . We did not go further, because for  $L = 32$  and the maximum available  $m$  (actually 120), the relative error on the current was already 5% in the non-interacting case. It is nevertheless satisfactory to see that the results are again consistent with the extrapolation of the exact diagonalization data, as shown in Figure 4.

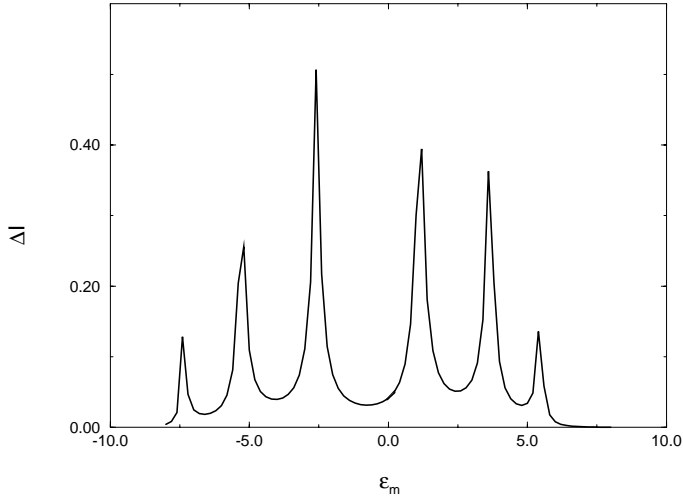


**Fig. 5.** Plot of the average persistent current  $I$  versus the molecular potential in the interacting case for  $V/t = 1$ . This curve has the same general shape as  $I(\epsilon_m)$  in the non-interacting case. Here  $M = 6$ ,  $L = 18$ ,  $t_1 = 2.6t$ ,  $t_2 = 2.2t$ ,  $\alpha = 0.3t$ .

## 4.4 Results

### 4.4.1 Variation of $\Delta I$ with $\epsilon_m$

The plot of  $\Delta I$  versus  $\epsilon_m$  (Fig. 5) for a half-filled ring has the same shape as in the non-interacting case (Fig. 3). The main effect of the interaction is to shift the location  $\epsilon_m^{min}$  and the value  $I_{min}$  of the minimum current. But the 6 resonances are still present, although their relative distances change with respect to the non-interacting case. The current  $I_{min}$  is the one we are interested in. And the corresponding  $\epsilon_m^{min}$  does not change with  $L$ , but depends on  $V$  (it is roughly equal to the opposite of  $V$ ):  $\epsilon_m^{min}$  counterbalances the mean field effect of  $V$ .

### 4.4.2 Effect of $V$ on $I$ for a given gap

In order to study the effect of electron-electron interaction on the minimum current, we have to find a meaningful way to compare it to the non-interacting case. Now, in a realistic situation, the rough value of the hopping integrals  $t_1$  and  $t_2$  is usually known — it is basically given by the total bandwidth  $2(t_1 + t_2)$  — but the precise value of their ratio, which together with the interaction term controls the charge gap  $\Delta_c$ , is not known as accurately. The gap itself is known quite accurately however. So we have decided to compare models with the same values of  $2(t_1 + t_2)$  and  $\Delta_c$ . In a given class of models,  $V$  is then a function of  $t_2/t_1$ .

The main result of this paper is that, for a given bandwidth and a given charge gap  $\Delta_c$ , the minimum persistent current  $I_{min}$  is larger when the interaction is partially responsible for the charge gap than when the charge gap is due only to the dimerization. If we plot  $I_{min}$  versus  $V$  for fixed  $\Delta_c$  and bandwidth, as in Figure 6, this effect appears clearly, and it is quite substantial. For example, if

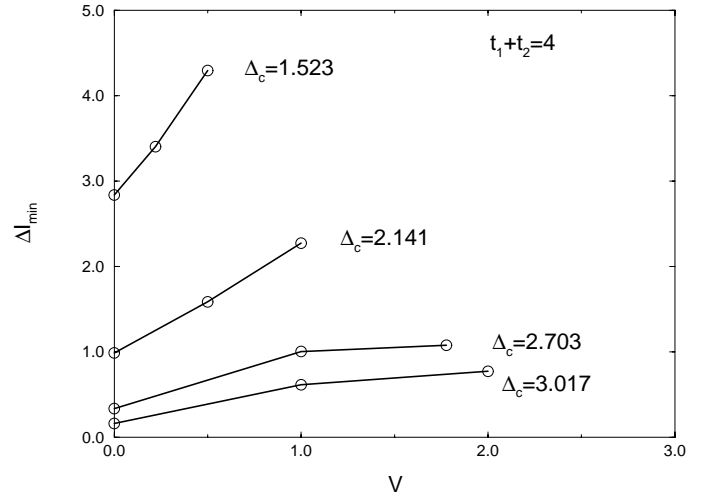


**Fig. 6.** Plot of the minimum of the persistent current  $\Delta I_{min}$  versus the repulsion  $V$  for fixed charge gap and bandwidth.

$2(t_1 + t_2) = 4t$  and  $\Delta_c = 3.02t$  we get a current twice as large for  $V = t$  than in the non-interacting case. Note in Figure 6 that each curve is limited to the right since there is a maximum value of  $V$  consistent with each given gap.

In fact, if we plot the current versus the repulsion for given bands, it decreases from  $I_0$  to  $I_1$  by turning on the repulsion. But this repulsion also increases strongly the gap. And the noninteracting system having this new gap has a current much lower than  $I_1$ . This is why the effect of the interaction for a fixed gap favours the tunneling of electrons through the molecule.

### 4.4.3 Influence of the molecule's length

The results of the previous subsection can be extended to  $M = 8$  and  $M = 10$ . As mentioned in the Introduction, the current decreases exponentially with the length of the molecule in the non-interacting case. We find that for various parameters (repulsion, bandwidth, dimerisation), this exponential behavior still holds for interacting particles, as shown in Figure 7.

If we choose a set of parameters and consider the equivalent, non-interacting system (same gap, same bandwidth), this system turns out to depend only very slightly on the size. Therefore, the corresponding current decreases exponentially with  $M$ . And we find that the coefficient of this exponential is larger than in the interacting case. (In Fig. 7 it is given by the slope of the lines.) In other words, the current is not only larger when interactions are present for a given size, but the exponential decrease with respect to the length of the molecule is slower in the interacting case as well. This is very important since it is this exponential decrease that puts limitations on the use of long molecules as wires.

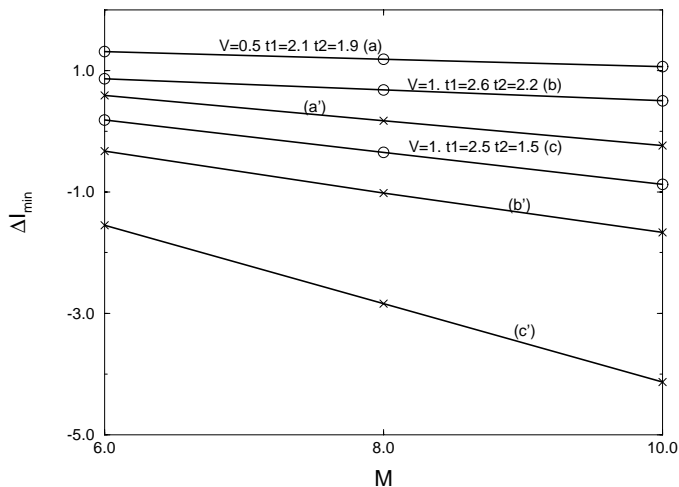


**Fig. 7.** Plot of the logarithm of  $\Delta I$  versus the size  $M$  of the molecule. For each interacting system (circle) the equivalent non-interacting system (same gap and band-width) is plotted with crosses. In each example, we get straight lines and the curve with interaction is above the corresponding one without interaction and decreases more slowly.

## 5 Conclusions

In this paper, our goal was to estimate the tunneling current through an interacting oligomere molecule, like polyene. The interaction turned out to play an important role. In this molecule, the charge gap can be reproduced by a dimerization and no interaction. This would correspond to a band insulator in the limit of an infinite molecule. This gap can also be reproduced by interactions and a smaller dimerization. Then we tend toward the Mott-Hubbard gap limit.

If we fix the band parameters, the charge gap increases when we turn on the interaction, and our numerical simulations show of course a decrease of the current. But for a given bandwidth, if we reduce the dimerization while we increase the interaction, in order to keep a constant charge gap, then the current grows. Thus a Mott-Hubbard gap is less damaging than a pure dimerization gap for the current. Furthermore, in the interacting case, the persistent current decreases exponentially with the size of the molecule, like in the non-interacting equivalent case, but more slowly. So, the above mentioned difference concerning the current between a Mott-Hubbard gap and a pure dimerization gap increases with the size of the molecule.

The next step will be to study the effect of the spin to check whether our results will hold for a realistic molecule with spin degrees of freedom. Clearly, they can already be applied to compounds where the on-site repulsion is strong compared to the other energy scales, and polyene is not so far from this situation, since  $t_1 \simeq 2.5$  eV,  $U \simeq 11.5$  eV and  $V \simeq 2.4$  eV. Whether this remains true for more general systems is left for future work.

We acknowledge very useful discussions with C. Bruder, C. Joachim and M. Magoga. We are especially indebted to C. Stafford for very useful explanations concerning persistent currents, and E. Sorensen for his help with the DMRG. The numerical simulations have been performed on the C94 and C98 of the IDRIS.

## References

1. R. Landauer, *Philos. Mag.* **21**, 863 (1970).
2. D. Stone, A. Szafer, *IBM J. Res. Develop.* **32**, 3 (1988).
3. C. Joachim, J.F. Vinuesa, *Europhys. Lett.* **635**, 33 (1996).
4. C. Joachim, J.K. Gimzewski, R. Schlittler, C. Chavy, *Phys. Rev. Lett.* **74**, 2102 (1995).
5. M. Magoga, C. Joachim, *Phys. Rev. B* **58**, 4722 (1997).
6. D. Baeriswyl, *Synth. Met.* **57**, 4213 (1993).
7. Z.G. Soos, G.W. Hayden, *Electroresponsive Molecular and Polymeric Systems*, edited by T.A. Skotheim (Dekker, New York, 1988), p. 197.
8. H. Thomann, L.R. Dalton, *Handbook of Conducting Polymers*, edited by T. Skotheim (Marcel Dekker, New York 1986), p. 1157.
9. P.K. Kahol, G.C. Clark, M. Mehring, *Conjugated Conducting Polymers*, edited by H. Kiess, *Springers Series in Solid-State Science* **102**, 217 (1992).
10. J.E. Hirsch, M. Grabowski, *Phys. Rev. Lett.* **52**, 1713 (1984).
11. R.H. Friend, D.D.C. Bradley, P.D. Townsend, *J. Phys. D* **20**, 1367 (1987).
12. D. Baeriswyl, D.K. Campbell, S. Mazumdar, *Phys. Rev. Lett.* **56**, 1509 (1986).
13. P. Fulde, *Electron Correlations in Molecules and Solids* (Springer Verlag, 1993), p. 172.
14. I. Safi, H.J. Schulz, *Phys. Rev. B* **52**, R17040 (1995); I. Safi, *Phys. Rev. B* **55**, R7332 (1997).
15. D. Maslov, M. Stone, *Phys. Rev. B* **52**, R5539 (1995).
16. Y. Meir, N.S. Wingreen, *Phys. Rev. Lett.* **68**, 2512 (1992).
17. V. Mujica, M. Kemp, M.A. Ratner, *J. Chem. Phys.* **101**, 6849 (1994).
18. S.R. White, *Phys. Rev. B* **48**, 10345 (1993).